AD-A137 531 ELECTRONIC SPECTRA OF CONDENSED PHASE UNDER SHOCK CONDITIONS(U) WASHINGTON STATE UNIV PULLMAN SHOCK DYNAMICS LAB G E DUVALL AUG 83 N00014-77-C-0232 1/1

UNCLASSIFIED F/G 20/4 NL

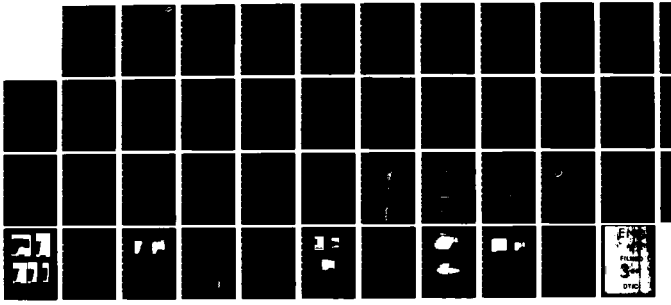

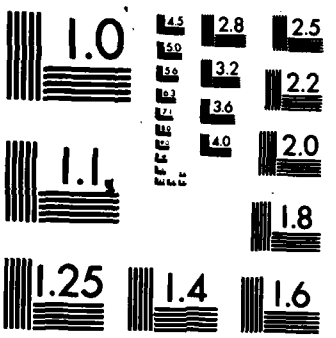

MICROCOPY RESOLUTION TEST CHART
NATIONAL BUREAU OF STANDARDS-1963-A

SECURITY CLASSIFICATION OF THIS PAGE (When Data Entered)

REPORT DOCUMENTATION PAGE

READ INSTRUCTIONS BEFORE COMPLETING FORM

1. REPORT NUMBER	2. GOVT ACCESSION NO. AD-A137531
3. RECIPIENT'S CATALOG NUMBER	
4. TITLE (and Subtitle) Electronic Spectra of Condensed Phase Under Shock Conditions	5. TYPE OF REPORT & PERIOD COVERED ~~Technical~~, 7/1/82 - 6/30/83
	6. PERFORMING ORG. REPORT NUMBER
7. AUTHOR(s) G. E. Duvall, Principal Investigator	8. CONTRACT OR GRANT NUMBER(s) N00014-77-C-0232
9. PERFORMING ORGANIZATION NAME AND ADDRESS Physics Department, Shock Dynamics Lab Washington State University Pullman, WA 99164-2814	10. PROGRAM ELEMENT, PROJECT, TASK AREA & WORK UNIT NUMBERS
11. CONTROLLING OFFICE NAME AND ADDRESS Office of Naval Research 800 N. Quincy Street Arlington, VA 22217	12. REPORT DATE August 1983
	13. NUMBER OF PAGES
14. MONITORING AGENCY NAME & ADDRESS(if different from Controlling Office) Office of Naval Research, Resident Representative University District Bldg, Rm 422 1107 NE 45th Street Seattle, WA 98195	15. SECURITY CLASS. (of this report) UNCLASSIFIED
	15a. DECLASSIFICATION/DOWNGRADING SCHEDULE

16. DISTRIBUTION STATEMENT (of this Report)

Approved for public release; distribution unlimited

17. DISTRIBUTION STATEMENT (of the abstract entered in Block 20, if different from Report)

18. SUPPLEMENTARY NOTES

19. KEY WORDS (Continue on reverse side if necessary and identify by block number)

Shock Waves
Condensed Matter
Carbon Disulfide
Decomposition
Spectroscopy

20. ABSTRACT (Continue on reverse side if necessary and identify by block number)

DD FORM 1 JAN 73 1473

SECURITY CLASSIFICATION OF THIS PAGE (When Data Entered)

ANNUAL SUMMARY REPORT
07/01/82 - 06/30/83

George E. Duvall
Principal Investigator
Department of Physics
Shock Dynamics Laboratory
Washington State University
Pullman, WA 99164-2814

Office of Naval Research
Contract Number N00014-77-C-0232
Washington State University Control Number
11F-2464-0058

December 6. 1983

Foreword

The work described here has been carried out principally by Richard Granholm, P. M. Bellamy, Dr. Richard Wilson, Robin Collins, and Peter Eschbach, with advice and assistance from other faculty, students and staff in the Shock Dynamics Laboratory. Results shown are preliminary and quantitative data are subject to change before publication.

I. INTRODUCTION

Chemical reactions in condensed matter inevitably involve continuum mechanics and thermodynamics. When the reactions are exothermic and fast, large amplitude wave propagation is involved and the relations among the aforementioned processes are so intimate that cause and effect are difficult to separate--passage of the shock wave initiates the reaction and the reaction drives the shock wave. Both the shock wave and the reaction influence the temperature history of a mass element participating in the reaction.

Detonation is the best known example of such a reaction. It has been studied for over a hundred years, but most effort has gone into understanding continuum mechanics aspects, with moderately sophisticated thermodynamics, primitive treatment of chemical reaction theory, and almost no attention to molecular processes. In consequence, progress in understanding the total reaction phenomenon has been slow.

During the last 30 years a substantial amount of information has accumulated on non-explosive reaction in shock waves. This work has been done in Australia, Japan, the U.S.A., and the Soviet Union. It suggests that the effect of a shock wave in producing chemical reactions goes beyond the simple effects of pressure and temperature. There may

be direct interaction between the shock front and the individual molecules which influences their chemical states. There are certainly large numbers of structural defects produced in the shock, and these may serve as nucleation centers for initiation of reactions, or they may otherwise affect the course of the reaction.

There are also large, heterogeneous electric fields and charge distributions in insulating solids, and probably in liquids too. These may be expected to be altered in the shock front and to contribute to the total reaction process.

Plausible mechanisms of direct interaction between shock front and molecules include direct transfer of energy to particular modes, molecular deformation through impact, and torsion of large molecules. Such interactions are strongly dependent on rise time in the initiating shock, which may be the order of 10^{-12} seconds in some circumstances.

Research being conducted under this contract addresses the above problems directly using the best diagnostic technique presently available which is suited to the shock environment, viz., optical spectroscopy in the visible and UV regions. The subject material to date has been principally liquid carbon disulfide. The principal emphasis has been on identifying spectroscopic features which are sensi-

tive to compression and searching for evidence of the dependence of these features on the rate of compression and for evidence of "catastrophic" shock effects. The principal finding has been that the wavelength of the red edge of the 3200 Å absorption band in carbon disulfide is remarkably sensitive to dynamic compression. Considerable effort has gone into characterizing this effect, as will be seen in the following sections.

II. EXPERIMENTAL PROCEDURES

Figure 1 is a drawing of the fifty foot gas gun used to produce shock waves in the sample. The breech containing high pressure nitrogen or helium and the projectile is at the left, and the muzzle, target chamber, and catcher tank are at the right. The design of this gun is novel inasmuchas both barrel and breech are free to slide on bronze pads and the recoil is absorbed by large shock absorbers, shown just to the right of the breech. The standard projectile is 4 inches in diameter, 8 inches long, and weighs 2 pounds. Its velocity can be varied between 200 and 1300 meters per second. The higher velocity is enough to produce a 300 kilobar shock in sapphire-sapphire impact. The best time resolution achieved in experiments with this facility has been about 5 nanoseconds, and observation time varies from 0.5 to about 5 microseconds, depending on the experiment.

The sample is contained in a target cell mounted in a fixture at the end of the barrel and inside the muzzle room, shown at the right side of Fig. 1. Measurement of spectra involves a sequence of events initiated by trigger pins situated in the target and by impact of the projectile face with the target face. The required light source is a xenon flash lamp. Light transmitted by or reflected from the sample is dispersed by means of a grating spectrograph, and the

resulting spectrum is spread over time and recorded using either an electronic or rotating mirror streak camera. Two kinds of measurement can be made, reflection and transmission. The configurations of projectile and target used for these measurements are shown schematicaly in Figs. 2 and 3.

The sample is contained in a cell consisting of a cylindrical brass housing containing two sapphire disks with axes coaxial with the housing. The penny-shaped cavity between the disks is filled with the sample liquid. The cells are shocked by impacting one face of the cell with a sapphire disk of the same diameter mounted in a 10.2 cm diameter projectile. The front, or impact face, of the cell is approximately 3 mm thick and the back is about 12.7 mm thick. The sample cavity thickness varies from less than 1 to about 170 microns.

Two basic variations of the experiments are used. The first, for reflection experiments, is shown in Fig. 2. Light from a xenon flashlamp is focussed into the back of the cell. A mirror is placed at the back of the impactor so that the mirror remains unshocked for the duration of the experiment. The intent is that the light should pass through the cell and impactor, reflect from the mirror, then pass through the impactor and cell a second time. The light from the cell is directed to the spectrograph by means of a mirror mounted behind the target, as shown in the figure. A

6 degree tilt on the rear face of the back sapphire disk prevents reflections from this surface from reaching the dispersion unit and streak camera.

The arrangement for transmission experiments, is shown in Fig. 3. In the first set of transmission experiments, the flashlamp was mounted in the projectile, as shown, and power was transmitted to it through electrical contacts closed by impact. In the present form of the experiment the flashlamp is mounted in the target, as shown in Fig. 4.

Impact pressure, i.e., final pressure reached in the sample, is controlled by adjusting the projectile velocity. The head of the projectile is of 6061-T6 aluminum, 0.5" thick. On the face is mounted an aluminum cylinder with a slot in it. This supports a 0.5" thick sapphire impactor approximately 1" in diameter. Between the sapphire and the projectile face is a front surface mirror mounted at a 45 degree angle in order to direct light from the xenon flash-lamp through the impacting sapphire. The target and flash-lamp are shown at the right of Fig. 4. The flash lamp is made in the form of a circular arc in order to accomodate any rotation of the projectile which may occur. It extends beyond the surface of the target so that there is a clear optical path from the lamp to the 45 degree relay mirror and through the center of the impactor and sample cell for the duration of the experiment. The lamp is driven by a 15,000

volt, 2 microfarad power supply. The latter is triggered by a pin extending out from the target and shorted by the projectile face approximately 4.2 microseconds (i.e., 2 mm) before the impactor in the projectile strikes the front face of the cell, labelled "F" in the drawing. The lamp reaches full brightness 3.3 microseconds after the power supply is triggered.

The sample is contained in a narrow gap between two pieces of sapphire or quartz, labelled "F" and "B" in the drawing. In the standard cell, the shock wave reaches the sample 275 nanoseconds after impact. The shock impedance of the sample is much less than that of the sapphire, so the amplitude of the first shock in the sample is only about 10 percent of the impact pressure, P_i. The pressure in the sample "rings up" to the impact pressure through a succession of reflected shock waves which reverberate between the sapphire surfaces bounding the sample. Time for pressure in the sample to ringup depends on its thickness. It ranges from about 2 nanoseconds for 1 micron thick cells to about 300 nanoseconds for 150 micron cells.

The ringing up process for a 145 micron cell with impact (final) pressure of 55 kilobars is shown in Fig. 5, and the pressure-time relation for the sample is shown in Fig. 6. In Fig. 5a, the shock is incident on the carbon disulfide layer from the sapphire on the left. The first

shock in the carbon disulfide produces a state "1" behind it, shown as point 1 in the pressure-particle velocity plane, Fig. 5b. When this first shock reaches the back face of the sapphire, reflection in the carbon disulfide and transmission into the sapphire occurs, yielding state 2, etc. At the instant of each reflection the entire cell is at a uniform pressure, temperature and particle velocity. At intermediate times it is in a mixed state. As time and number of reverberations increase, pressure in the sample approaches impact pressure in the sapphire asymptotically, as shown in Fig. 6. The steps in this figure represent the times of reflection, as shown in Fig. 5, and the uniform pressure states which exist at those times. In order to distinguish this kind of compression loading from that produced by a single shock or by continuously increasing compression, it will be called "stepwise" or "SW" loading.

It is also possible to load the sample so that the pressure increases continuously in time over a limited range of time and pressure. This is accomplished by making the front face of the sample-holding cell from fused quartz. The compressibility of fused quartz increases with pressure, and this property causes a step increase in pressure generated by impact at one face to be converted to a ramp or continously rising wave, as it propagates (70BH).. The rise time of the wave when it reaches the sample is related to the thickness of the fused quartz by the equation:

$$t_r = h(c_o - c_1)/c_o c_1 \qquad (1)$$

where h is the uncompressed cell thickness; c_o is sound velocity at atmospheric pressure; and c_i is Lagrangian sound velocity at the impact pressure P_i (70BH):

$$P = 1.317 - 7.361u^2 + 99.47u^3 - 416.3u^4 \qquad (2a)$$

$$c = 0.59836 - 6.6888u + 135.579u^2 - 756.57u^3 \qquad (2b)$$

$$c = \frac{\rho}{\rho_o}\left(\frac{\partial P}{\partial \rho}\right)_s^{\frac{1}{2}} \quad \text{Lagranian sound velocity}$$

where P is pressure in megabars, u is particle velocity, and both u and c are expressed in cm per microsecond. The sample is contained between the fused quartz and a sapphire back plate. By making the sample very thin, the wave transit time through the sample can be made sufficiently small that the sample is essentially free from pressure and temperature discontinuities. This has been called "Dynamic Isentropic Compression" or "DIC", and will be so referred to here.

In the simplest approximation to pressure history of the sample in DIC, characteristics in both the h-t plane and the pressure-particle velocity (P, U_p) planes can be treated as straight lines, as shown in Fig. 7. In this figure, h is the initial uncompressed position of a plane which is parallel to the wavefronts. A shock is generated at O and the negative curvature of the P-V isentrope in fused quartz spreads it into a compression fan as shown. The successive states 11, 12, 13 are represented as points

in the $P - U_p$ plane. The states induced in the sapphire, and therefore existing at the interface at successive times, are denoted 21, 32, 43 on the sapphire Hugoniot curve and in the sapphire. If the pressure incident on the interface AB is $P_o(t)$, the pressure at the interface, including the effects of reflection, is then,

$$P_1(t) = P_o(t)[1 + (z_2 - z_1)/(z_2 + z_1)] \quad (3)$$

where z_2 and z_1 are the acoustic impedances of sapphire and fused quartz, respectively. z_2 for sapphire is nearly constant over a substantial range of pressure:

$$z_2 = 432 \text{ kb } \mu\text{sec/mm} \quad (4)$$

The impedance of fused quartz, z_1 , varies from about 131 to 116 kbar microsec/mm as pressure varies from 0 to 25 kbar. If an intermediate value is chosen for z_1, the resulting error for $P_1(t)$ is less than 5 percent.

The effect of the finite sample thickness at the interface can be accounted for approximately if $P_1(t)$ is replaced by $P_1(t+a)$ where a is ringup time in the carbon disulfide. The appropriate value of a is difficult to estimate, but it appears to be the order of 3 nanoseconds for a 1 micron thick sample. Shocking up of the ramp in the carbon disulfide is a problem if rise time of the ramp is

small and sample thickness is too large. Sample thicknesses have been chosen with this in mind. The DIC loading curve for a thin cell of carbon disulfide faced with a 0.45 inch thick piece of fused quartz is shown in Fig. 8. The impact pressure for this case was 27 kbar.

III. EXPERIMENTAL RESULTS

Experiments completed during this period are listed in Table I. They are collected into five groups, according to the purpose of the experiments. The principal measurement was the shift, $\Delta\lambda$, in the red band edge as a function of applied pressure for various conditions. Cells are described as "thick" (greater than 100 microns thick) or "thin" (less than 10 micron thick).

III.1 $\Delta\lambda$ VS Pressure for SW Loading in Thick cells of Carbon Disulfide

A. Initial Sample At Room Temperature, Group 1 Experiments

Spectrograms for impact pressures ranging from 55 kbars to 134 kbars are shown in Fig. 9. The light regions represent transmission; dark regions are regions of light extinction. Wavelength for each spectrogram increases vertically.

Time increases from left to right. The sequence of events can be described with the help of the labels in Fig. 9a.

The line of demarcation between black and white labelled OS represents the red edge of the 3200 Å absorption band in the undisturbed state of liquid carbon disulfide at room temperature and one atmosphere pressure. The exact wave length at which OS is seen depends somewhat on

film exposure and cell thickness. Impact of the projectile with the front face of the target sapphire occurs approximately 275 nanoseconds to the left of the corner marked S. The jump in band edge at S occurs when the first shock wave enters the carbon disulfide (h=Ø, t=Ø in Fig. 5a). The jump at J occurs when the first shock reaches the back side of the carbon disulfide sample. Rounding is caused by the finite time and spectral resolution of the spectrograph and streak camera instrument. Pressure nears its final value in the region marked A, and is constant until lateral rarefactions encroach on the central part of the cell at approximately F. Events following F involve changing pressures and non-uniaxial strains.

The record from shot number 82-Ø15 is not included in Fig. 9 because the absorption edge was shifted off the upper edge of the film. That from 82-Ø39 was omitted because of its similarity to 83-Ø14. The first three records, with final pressures, P_i, of 55, 77, and 84 kilobars, all have the same character.* The first two or three jumps in the absorption edge wavelength, $\Delta\lambda$, resulting from step increases in pressure can be followed at first. As pressure increases, $\Delta\lambda$ increases until pressure nears its final value in the corner of the "hook" (A in Fig. 9a). $\Delta\lambda$ then decreases slowly and somewhat irregularly for reasons not

* This is not evident in Fig. 9c. Exposure is less than for (a) and (b) and the copier failed to reproduce the less exposed part of the record.

well understood. In Fig. 9c, $\Delta\lambda$ increases further and the light intensity at longer wave lengths is diminished at late times. For the last two records, where P_i = 93 and 134 kilobars, respectively, $\Delta\lambda$ does not decrease during the time P is approximately constant. It increases instead, and more rapidly at the higher pressure than at 93 kilobars. We presume, at present, that this complete cutoff for large impact pressures represents a terminal reaction of the carbon disulfide, perhaps with the formation of free carbon (77YYD).

The records from all experiments have been analyzed by measuring $\Delta\lambda$ vs time from the original filmstrips. Pressure in the carbon disulfide has been calculated using a computer program called SHOCKUP which determines states 1, 2, 3, . . . shown in Fig. 5b. It is based on the Sheffield-1 Equation of State for liquid carbon disulfide and suitable Mie-Gruneisen approximations to the equations of state of the front and back plates of the cell (78S). When both P and $\Delta\lambda$ are plotted as functions of time, the steps in P and those in $\Delta\lambda$ should occur at the same time. Then P and $\Delta\lambda$ are well correlated and can be plotted with confidence in a graph like that shown in Fig. 10. The records of shots 82-018 and 82-039 do not offer a suitable correlation of P(t) and $\Delta\lambda$(t), so they are not represented in Fig. 10. A correlation can be established by varying cell thickness and impact pressure from the nominal values

given in Table I. It is not unreasonable to do this, since there are uncertainties in both cell thickness and projectile velocity, but it has not yet been done.

The data of Fig. 10 can be represented by the equations

$$\Delta\lambda(\text{Å}) = 27.0P - 0.277P^2 + 0.00238P^3 \quad P \text{ in kb} \qquad (5)$$

$$d\lambda/dP = 27.0 - 0.554P + 0.00714P^2 \quad \text{Å/kb} \qquad (6)$$

B. Effects of Changing Initial Temperature

Effects of varying the initial temperature of carbon disulfide were investigated in two experiments: Group 4 of Table I, and Fig. 11. The record of Fig. 11b is quite similar to those of Figs. 9a and 9b. The record of Fig. 11a at T_o = 125 C and 67 kb has the same character beyond this ringup time as that of Fig. 9d at 93 kb. This suggests that, if the late cutoff in 9d is due to decomposition, temperature plays a major role in the process.

In order to pursue this suggestion we must be able to separate temperature and pressure effects. This requires knowledge of temperature at various pressures and of the variation of $\Delta\lambda$ with T, independent of pressure. The analysis described below is intended to produce separate

values for pressure and temperature dependence of $\Delta\lambda$. Numerical values are indicative of the true situation, but somewhat suspect because of existing certainties in the CS_2 equation of state.

The effect of temperature on band edge under ambient pressure conditions has been measured in a standard cell at three different temperatures: -72°C, 25°C, 125°C. The cells were sealed, so pressure varied somewhat from one atmosphere as temperature changed, but the effect is small, estimated to be approximately 6 atmospheres at 125°C. Figure 12 shows spectrophotometer traces of light transmission for the three cases. The mean shift of the red edge with temperature under these conditions is

$$(\partial\lambda/\partial T)_{P_o} \simeq 0.4 \text{ Å/deg} \qquad (7)$$

When the samples at different initial temperatures were shocked and $\Delta\lambda$ was measured, the results shown in Fig. 13 were obtained. When the Sheffield-1 Equation of State is used to calculate temperature in the carbon disulfide, the ratio of $\Delta\lambda$ to ΔT at 40 kbar is found to be

$$\left(\overline{\partial\lambda/\partial T}\right)_{40} \approx 0.5 \text{ Å/deg} \tag{8}$$

With $\Delta\lambda \approx 800$ Å at 40 kb; $\Delta T = 400°C$, and $\left(\overline{\partial\lambda/\partial T}\right)$ given by Eq. (8),

$$\Delta\lambda = \left(\overline{\partial\lambda/\partial T}\right)\Delta T + \left(\overline{\partial\lambda/\partial P}\right)\Delta P \tag{9a}$$

$$\left(\overline{\partial\lambda/\partial P}\right)_{40} = [\Delta\lambda - \left(\overline{\partial\lambda/\partial T}\right)\Delta T]/\Delta P \tag{9b}$$

$$\approx 15 \text{ Å/kb}$$

The sensitivity of Eq. (9) to changes in $\left(\overline{\partial\lambda/\partial P}\right)$ is 1 Å/kb for a change of 0.1 Å/degree in $\overline{\partial\lambda/\partial T}$.

III.2 Δλ vs P for DIC Loading in Thin Cells of CS2

Figure 14 shows the spectrograms from three ramp loading (DIC) experiments listed as Group 2 of Table I. These have been analyzed using Eqs. (1) to (4) to obtain P(t). The results of the 338 nanosecond rise time shots are shown as curves OB and OD of Fig. 15. The 87 nanosecond ramp has not been plotted, but it lies on the curve OA within experimental error. The difference between OB and OD is attributed to cooling of the 1 μm thick cell in shot number 83-021.

III.3 Reflection Experiments in Carbon Disulfide, SW Loading

Figure 16 shows the spectrograms from two experiments using the arrangement of Fig. 2. The principal objective of these experiments was to determine whether or not the spectral range of large reflectivity corresponds to the spectral range of opacity in the transmission experiments. The preliminary conclusion is that there is at least an approximate correspondence.

Two features of these records are worth noting. One is that they contain transmission as well as reflection information. Analysis of these experiments is not complete, but the cutoff profile of Fig. 16b seems to lie on or close to the Δλ vs P curve of Fig. 10. The second is that the

reflection in Fig. 16b at 91 kbar is much more intense than the one at 60 kbar in Fig. 16a. This is true even at a time when pressure in 16b is considerably less than the final pressure in 16a. This suggests that the amplitude of the step discontinuities, shown in Fig. 6, play a major role in determining the reaction which causes reflection to occur.

III.4 Effects of SW Loading on Other Liquids

Spectrograms from a nitromethane (NM) experiment and from a mixture of carbon disulfide in ethanol are shown in Fig. 17. Impact pressure in the NM experiment is near the upper limit of our capability in an SW loading experiment because of loss of transparency of sapphire above about 130 kbar. NM is mechanically stiff compared to carbon disulfide. The band edge shift is nearly linear in time and it levels off at approximately 300 Å when pressure approaches its final value of 123 kbars. $\Delta\lambda$ vs temperature is linear to $P \approx 60$ kbar and is convex upward thereafter. Its dependence on pressure is initially concave upward, changing to convex upward for $P \gtrsim 90$ kbars. These features may result more from uncertainties in reading the records and in the equation of state than from true physical dependence. Pressures and temperatures were calculated from the Hardesty and Lysne equation of state for NM and checked with the Cowperthwaite and Shaw equation. Final temperature was approximately 740 K, far too low to react in the time of the experiment, according to Lysne and Hardesty.

A modified experiment of the Sheffield type was attempted with NM which would have increased temperature beyond 1000 K. It failed in two tries because of the failure of the impactor assembly on the projectile at large acceleration. Additional attempts will be made in the com-

ing year.

The experiment with diluted carbon disulfide was done for two reasons. One was to measure $\Delta\lambda$ for the isolated carbon disulfide molecule in order to obtain some idea of interaction effects. The other was to provide a direct comparison with the static pressure measurement of $\Delta\lambda$ made by Paul Schoen and colleagues at NRL. Results are shown in Fig. 15 as curve OC. Using the analysis of Eq. (9) with a Mie-Gruneisen form for the equation of state of the mixture gives

$$(\overline{\partial\lambda/\partial P})_{40\ kb} \approx 7\ \mathring{A}/kb$$

This curve of $\Delta\lambda$ vs P is in sharp contrast to the static measurement, shown as a point on the horizontal axis. The shift observed statically is small, if it exists at all, being less than about 15 $\mathring{A}$ at 10 kbar. The comparison is not entirely satisfactory because the absorption band in the static case simply becomes stronger and appears to broaden symmetrically, whereas in the dynamic measurements, the shift appears to occur primarily in the red edge.

An interesting feature of the spectrogram of Fig. 17b is the nearly bilinear nature of the cutoff curve. Pressure

becomes nearly constant at the point where the slope changes, but $\Delta\lambda$ continues to increase at a somewhat lower rate with time for the next 300 nanoseconds. This evidently represents the progress of a reaction, but whether it is occurring in carbon disulfide, in ethanol, or between the two is unknown at this time.

III.5 Electrical Measurements in SW Loaded Carbon Disulfide

Several resistance measurements have been made in modified versions of the cells shown in Fig. 2 and 3. There are detailed variations and unexplained details in the various measurements, but they all show that resistivity under compression drops by about 10 orders of magnitude to about 10^5 ohm cm and that there is no dramatic pressure dependence. There is some effect of light on resistivity and some evidence of electrode dependence, but these are not major effects.

Electrical polarization has been found to be induced by shock in carbon disulfide, but its magnitude is very small and would appear to have no role in the resistivity measurement.

IV. DISCUSSION

The work described here poses two questions: (i) Are the measurements accurate? (ii) What chemical mechanisms are responsible for the changes?

The first question is appropriate. The analysis required to arrive at curves of $\Delta\lambda$ vs P involves measurements of the position of the absorption band on the film and of the time at which it occurs. The absorption edge is not a step function in absorptivity, so the definition of its edge on film involves exposure time, film development and judgement on the part of the person reading the film as to the position of the edge. The best assurance of the accuracy of this measurement is that the scatter of readings by different individuals on the original film and on various facsimiles is relatively small. Pressure in the cell is obtained as a function of time by integrating the shock equations to find the intercepts at the cell boundaries shown in Fig. 5. This process depends on the equation of state of carbon disulfide and of sapphire. The latter is no problem. Until now, all of the calculations in carbon disulfide have been made using the equation of state developed by Sheffield and described in his thesis. It is called arbitrarily "Sheffield-1". It reproduces the Hugoniot P-V measurements in carbon disulfide very well and the Bridgman isotherms reasonably well. However, it does

contain a flaw which Sheffield has corrected in a recently published paper (83SD). Preliminary calculations show that P(t) agrees with the old equation, but temperatures are lower. Numbers presented here will be changed before final publication. The new equation of state (Sheffield-2) is still not entirely satisfactory--principally on esthetic grounds--and further studies will be made on the problem for this and other liquids.

Assurance that P vs t curves used to construct $\Delta\lambda$ vs P are correct comes from (i) correspondence in time between measured jumps in $\Delta\lambda$ and calculated jumps in P when reflection occurs at the carbon disulfide-sapphire interfaces, and (ii) from the overall coherence of the data as shown in Fig. 10. The comparison will be made sharper when time and spectral resolution are improved.

The second question on mechanisms goes to the heart of this research. Now that we have developed confidence in our measurements and have begun to build up a body of data, we can begin to explore various hypotheses more actively. Two suggestions are under consideration. One is that the shift in $\Delta\lambda$ is due to "hot bands" in the carbon disulfide. This implies that the carbon disulfide molecule is extracting energy from passage of the compression wave and storing it in vibrational states in amounts which exceed kT per mode for times of the order of 100 but not 300 nanoseconds (i.e.

the ramp shot results). This suggestion has some support from ultrasonic relaxation measurements, which give relaxation times as long as 30 nanoseconds for liquid carbon disulfide at normal ambient conditions. One would think that increasing the density would decrease the relaxation time, but there is no direct information on this point. A classical computation of this "hot band" effect does not indicate the kind of energy storage required to produce the observed values of $\Delta\lambda$. Recent consideration of this problem has shown the early calculation to have some flaws. Correction of these will change the earlier results in a direction to improve agreement with observation.

A second speculation arises from the results of the reflection experiments. These bespeak a substantial reflection coefficient, such as might be obtained from a poor metallic conductor. They are not explained by incoherent scattering because of geometry considerations. Rough calculation shows that both reflection and transmission measurements would be explained by formation of conducting platelets about 7 micron diameter and about 0.1 micron thick. It has been suggested that this could be due to formation of carbon sulfide polymer complexes, perhaps on the carbon disulfide-sapphire interfaces. However, no detailed model has been constructed. Experiments planned for the coming year may shed more light on this possibility.

V. PAPERS AND PUBLICATIONS

V.1 Papers Published

Optical Spectroscopy in a Shocked Liquid, G. E. Duvall, K. M. Ogilvie, R. Wilson, P. M. Bellamy and P. S. P. Wei, Nature 296 846-847 (1982).

Shock-Induced Changes in the Electronic Spectra of Liquid Carbon Disulfide, K. M. Ogilvie and G. E. Duvall, J. Chem. Phys. 78(3), 1077 (1983).

Response of Liquid Carbon Disulfide to Shock Compression: Equation of State at Normal and High Densities, S. A. Sheffield and G. E. Duvall, J. Chem. Phys. 79(4), 1981 (1983).

V.2 Presentations

The following talks were presented at the Third APS Topical Conference on Shock Waves in Condensed Matter, Sante Fe, NM (18-21 July 1983):

Electrical Properties of Shocked-Compressed Liquid Carbon Disulfide, R. Wilson and P. M. Bellamy.

Effects of Temperature on Light Extinction in Carbon Disulfide, R. H. Granholm, G. E. Duvall, and P. M. Bel-

lamy.

Light Extinction in Carbon Disulfide Compressed by Shock Reverberation, G. E. Duvall, R. H. Granholm, P. M. Bellamy.

A Projectile Cell, Light Source Combination Designed for Measuring Broad Band Transmission of Light in Shock Experiments, P. M. Bellamy.

VI. PARTICIPATING PERSONNEL

Paul Bellamy, Project Engineer

Richard Granholm, Research Assistant

Robert Wilson, Postdoctoral Research Assistant

Robin Collins, Undergraduate Student

Peter Eschbach, Undergraduate Student

REFERENCES

70BH L. Barker and R. Hollenbach, J. Appl. Phys. 41, 4208 (1970).

77YYD O. B. Yakusheva, V. V. Yakushev, and A. N. Dremin, Russ. J. Phys. Chem. 51, 973 (1977).

78S S. A. Sheffield, Ph.D. thesis, Washington State University (1978).

83SD S. A. Sheffield and G. E. Duvall, J. Chem. Phys. 78, 1077 (1983).

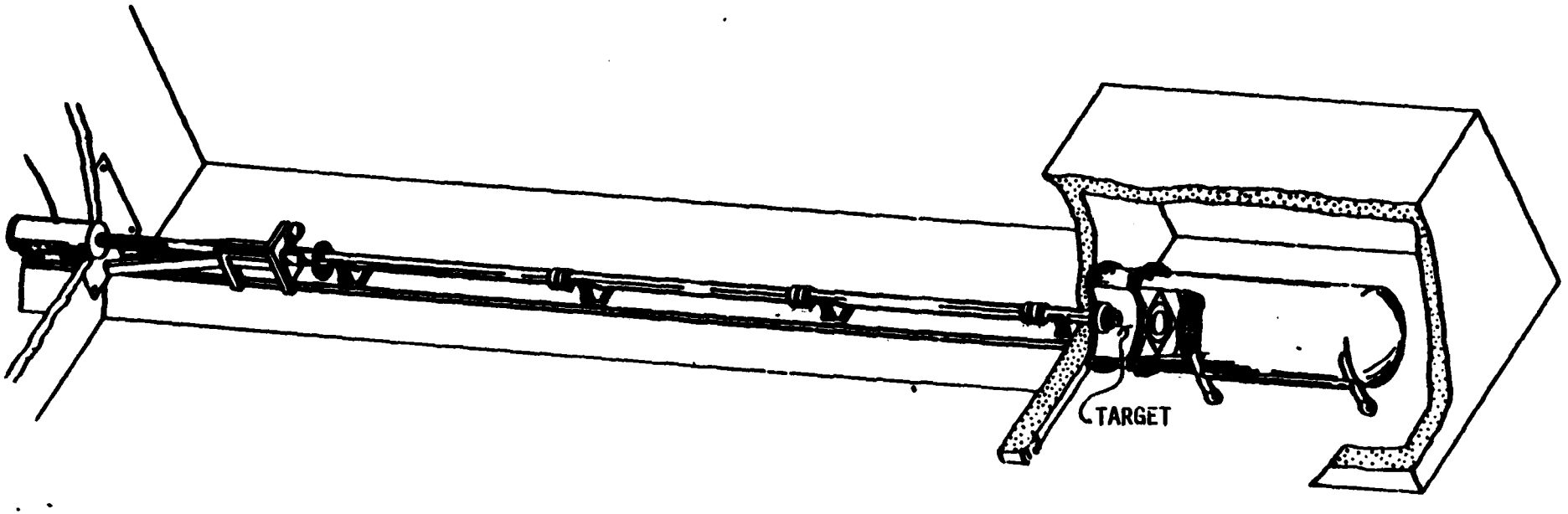

FIG. 1. Gas Gun and Catcher Tank Assembly

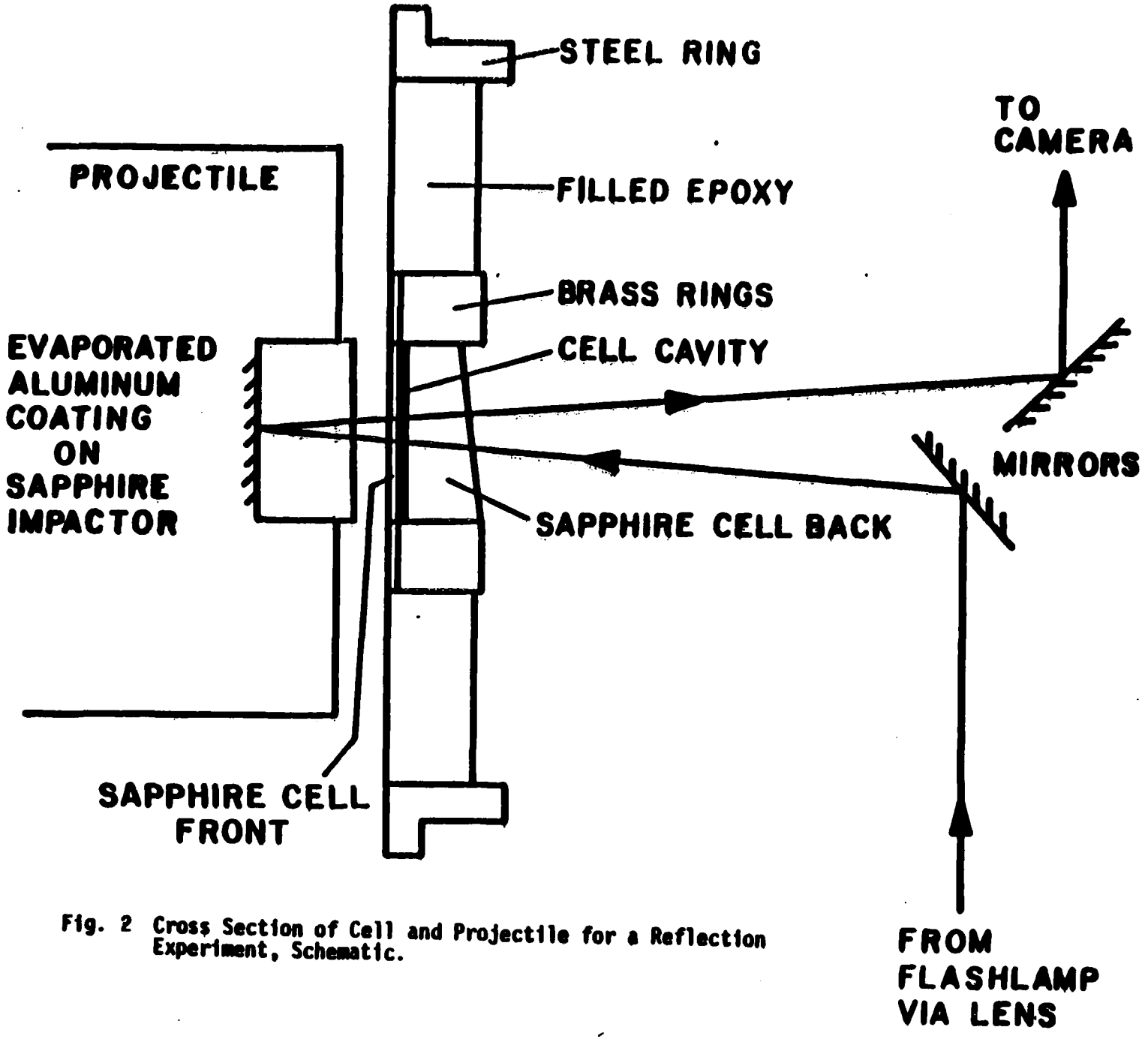

Fig. 2 Cross Section of Cell and Projectile for a Reflection Experiment, Schematic.

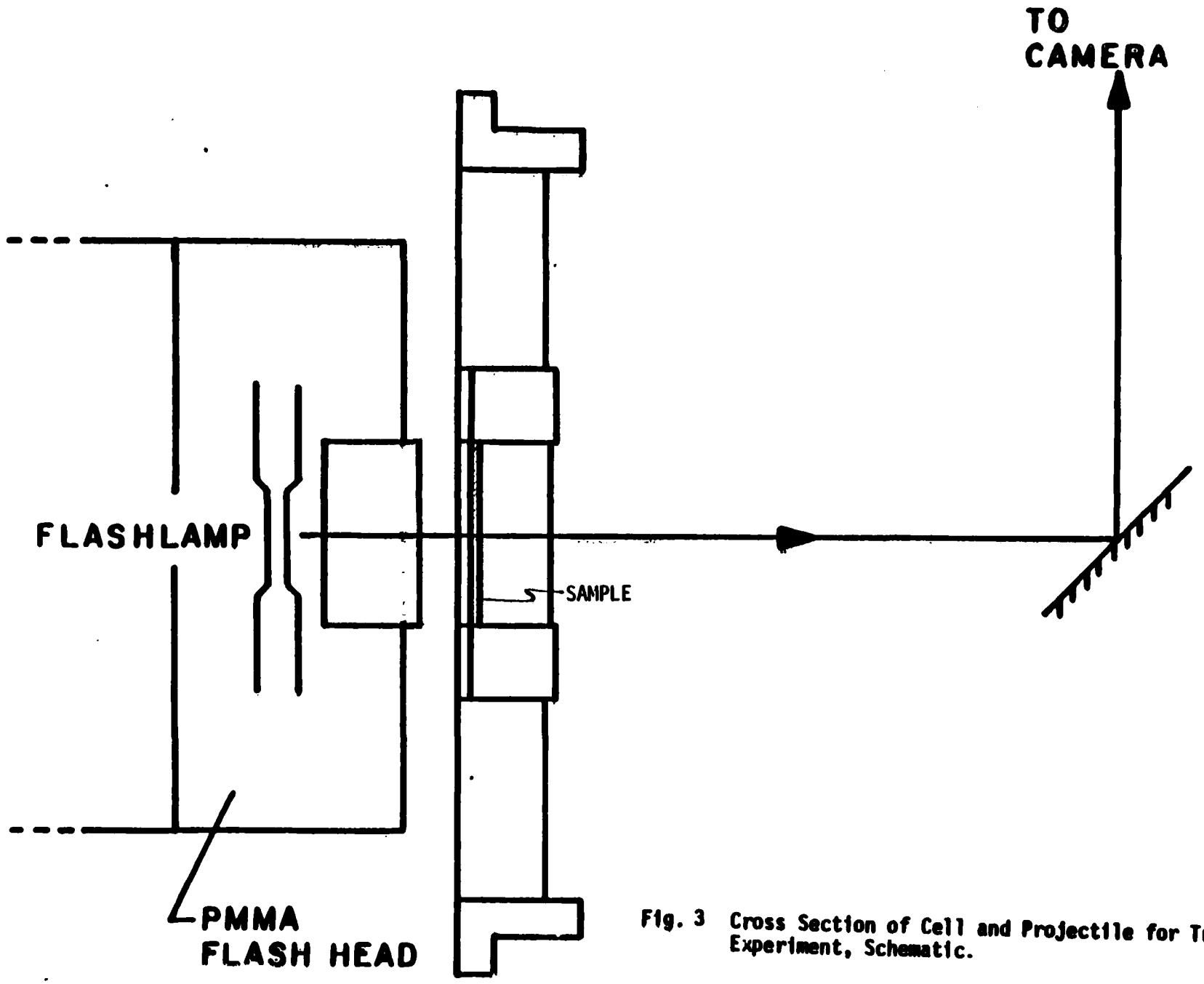

Fig. 3 Cross Section of Cell and Projectile for Transmission Experiment, Schematic.

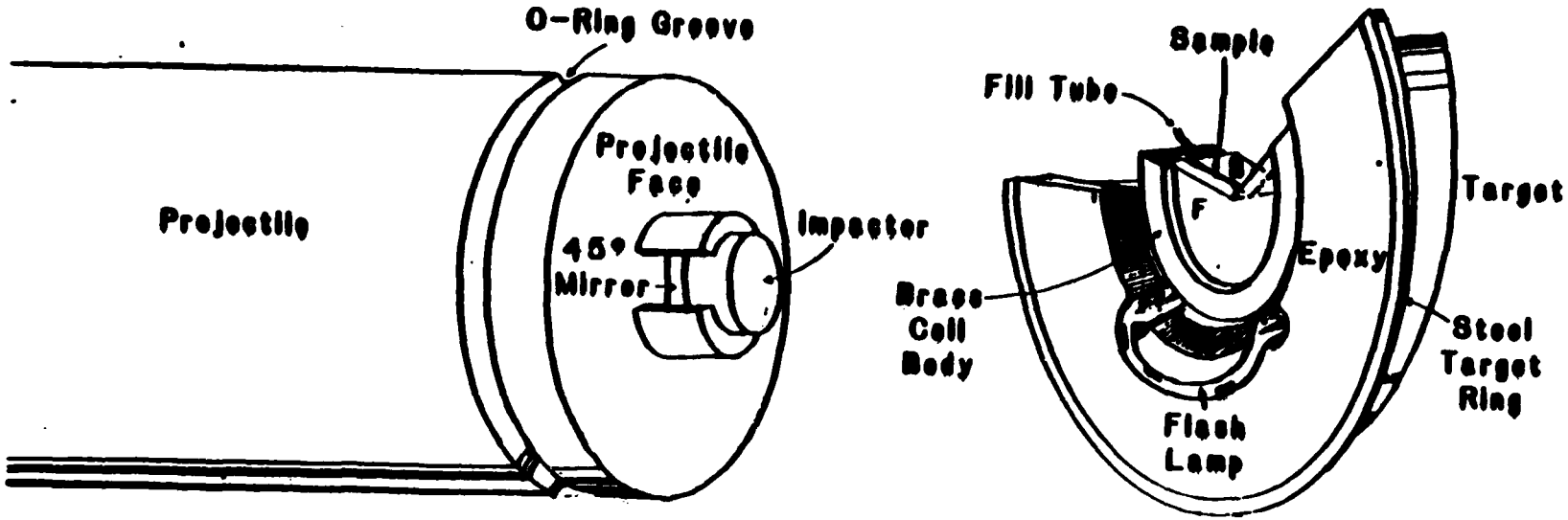

Fig. 4. Sketch of projectile and target for transmission measurements.

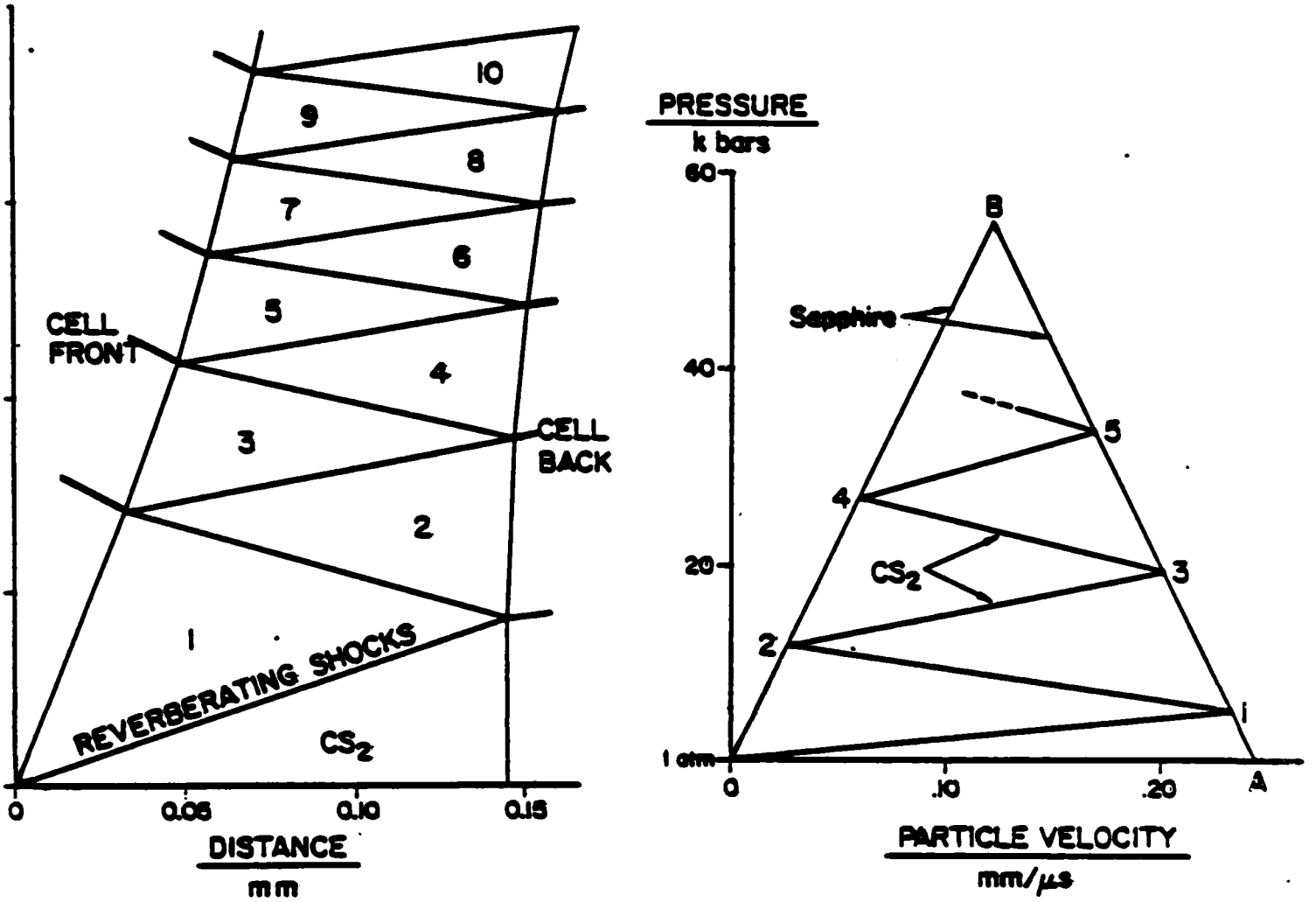

Fig. 5 Reverberations in a CS_2 Sample Confined Between Two Sapphire Plates.

(a) Shock front loci in the x-t plane;

(b) Successive states in the pressure-particle velocity plane.

Shot number 81-010, P_1 = 55 kbar.

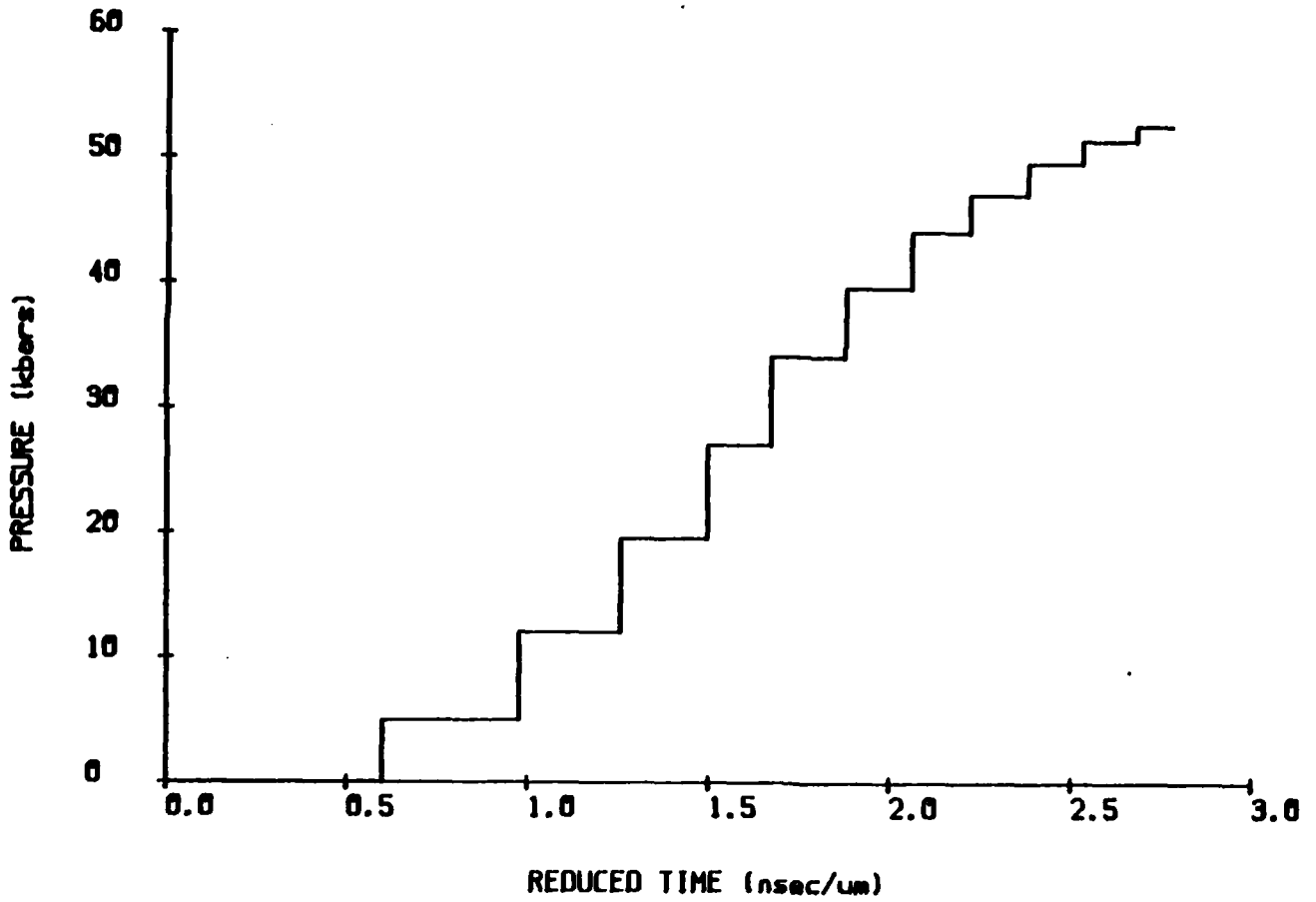

Fig. 6. Pressure history of CS_2 Cell shown in Fig. 5. Reduced time is time after shock enters CS_2. Cell thickness in μm.

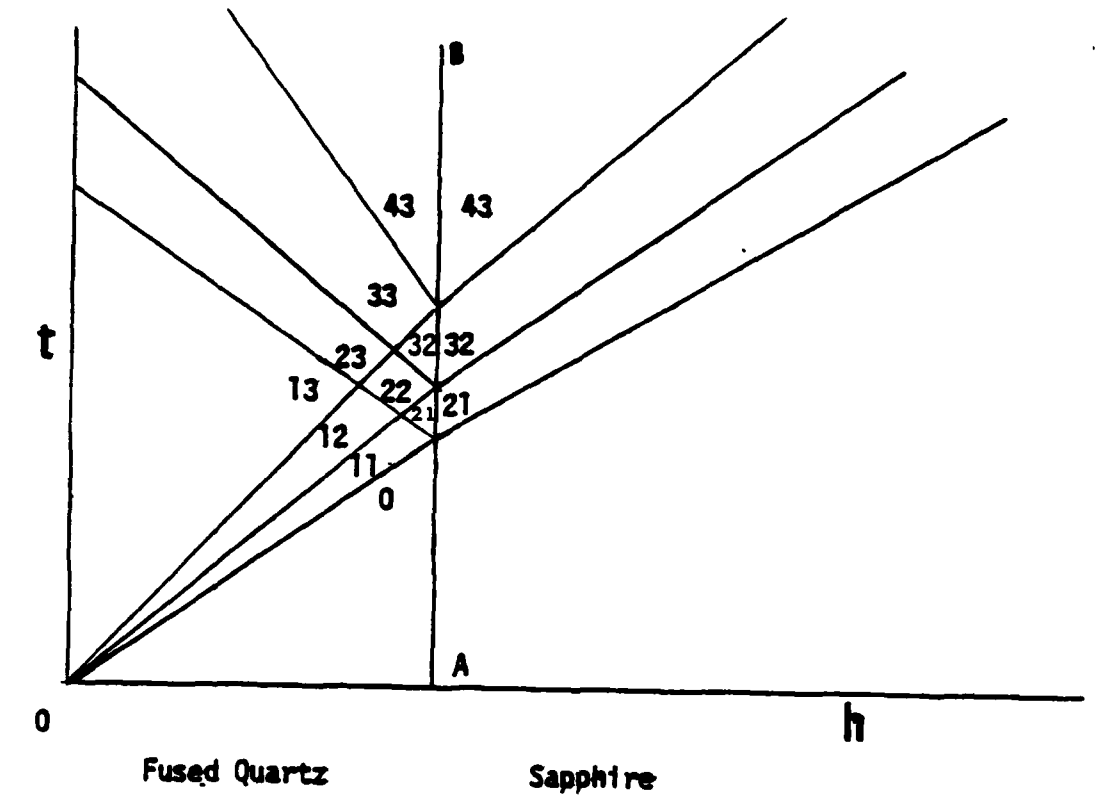

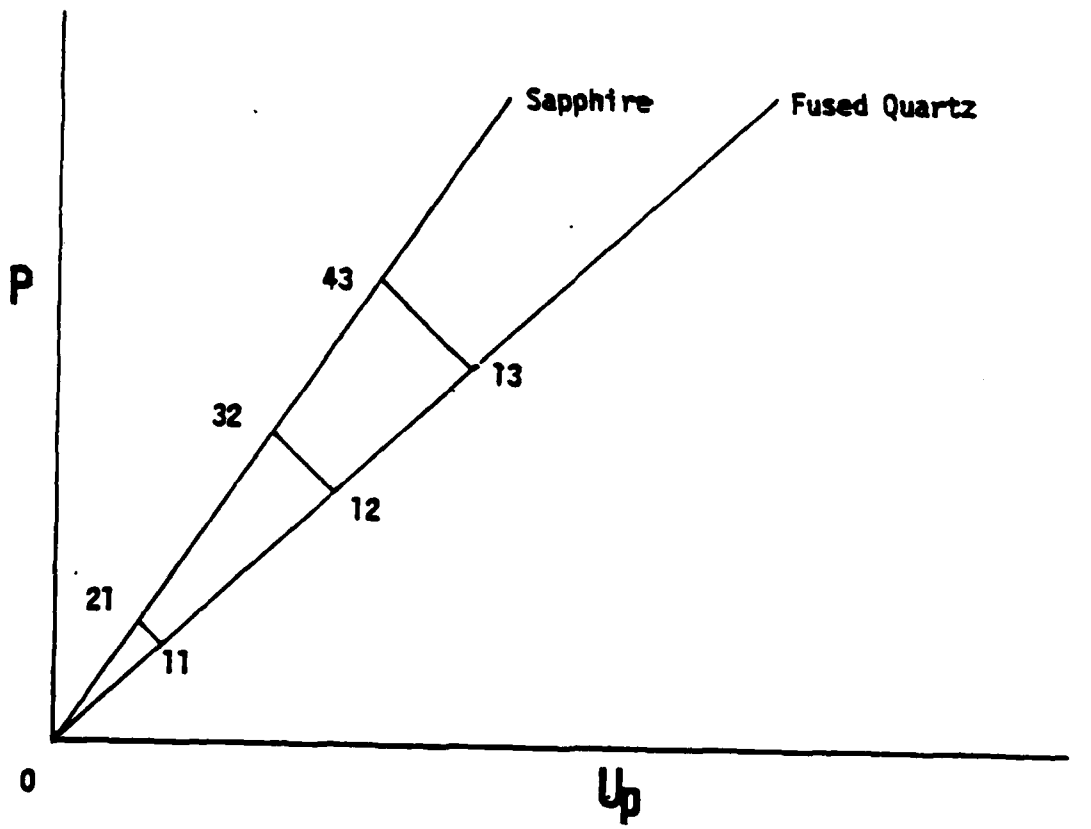

Fig. 7. Ramp Loading at a Fused Quartz-Sapphire Interface; Linear Approximation

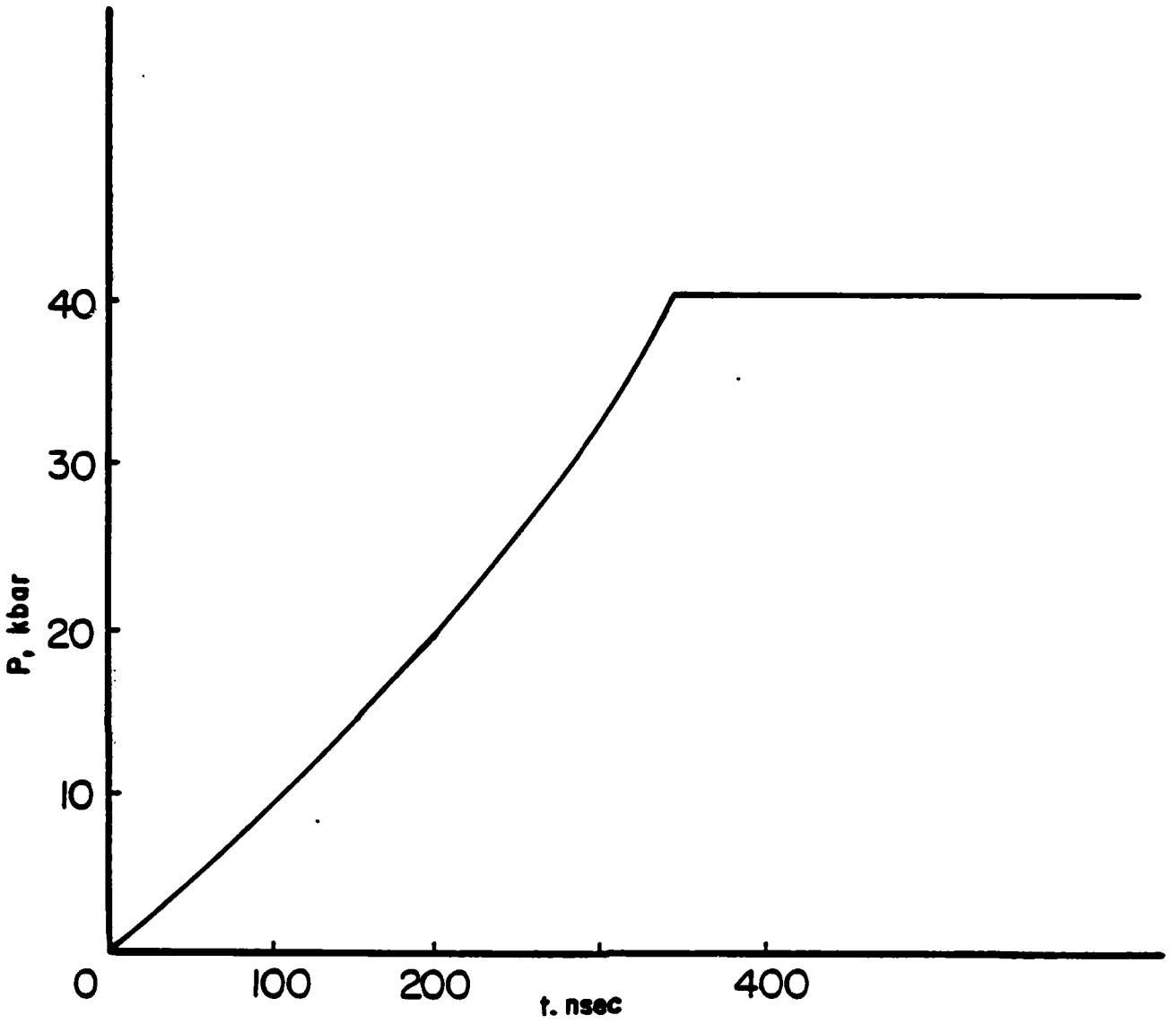

Fig. 8 P(t) for shots 83-021 and 83-042
Calculated by the methods of Fig. 7.

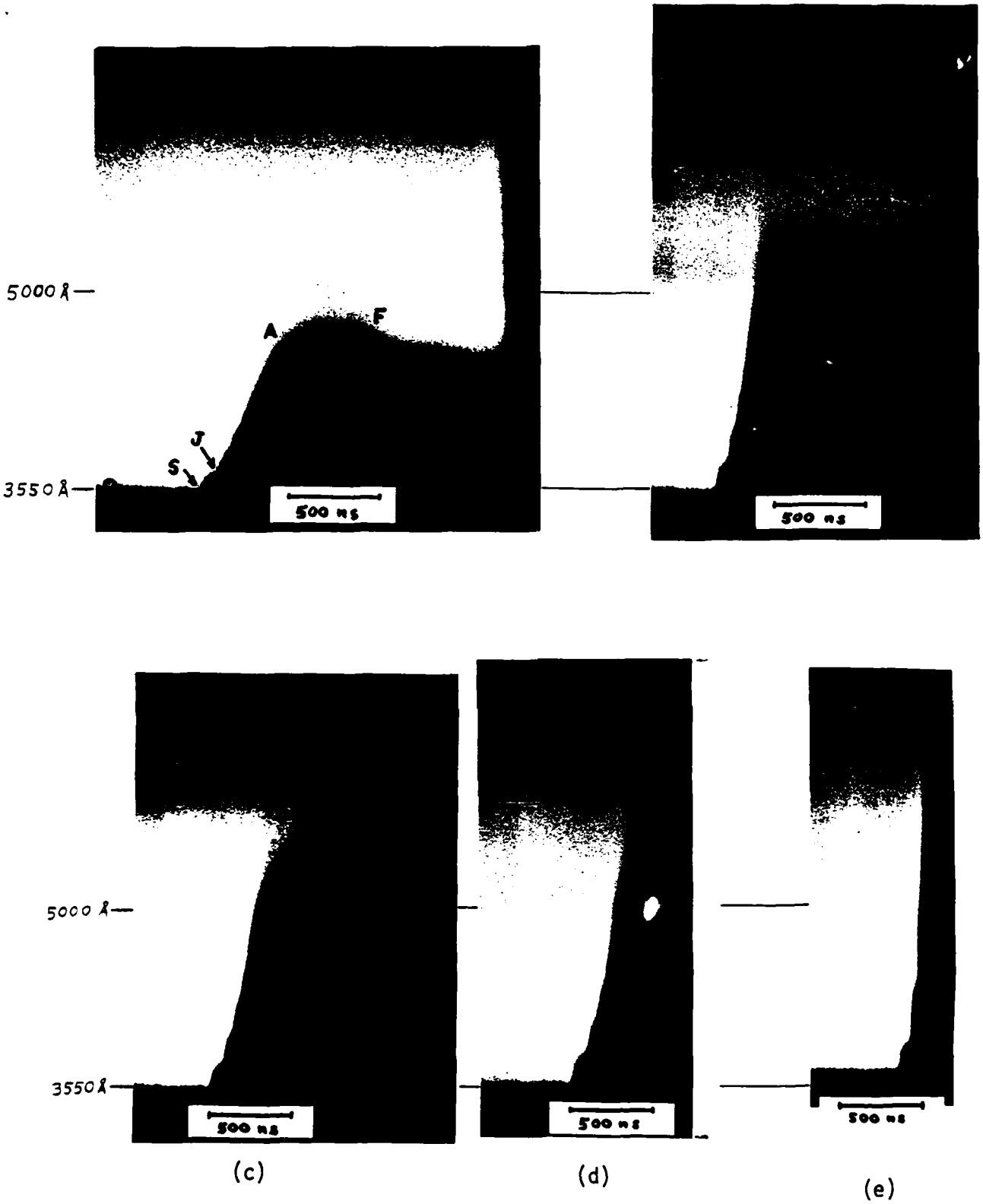

Fig. 9 Spectrograms showing transmission of light through liquid CS_2 before, during and after being subjected to stepwise loading. Group 1 of Table I, Final pressures: (a) 55 kb; (b) 77 kb; (c) 84 kb; (d) 93 kb; (e) 134 kb (with PMMA filter). Time increases from left to right.

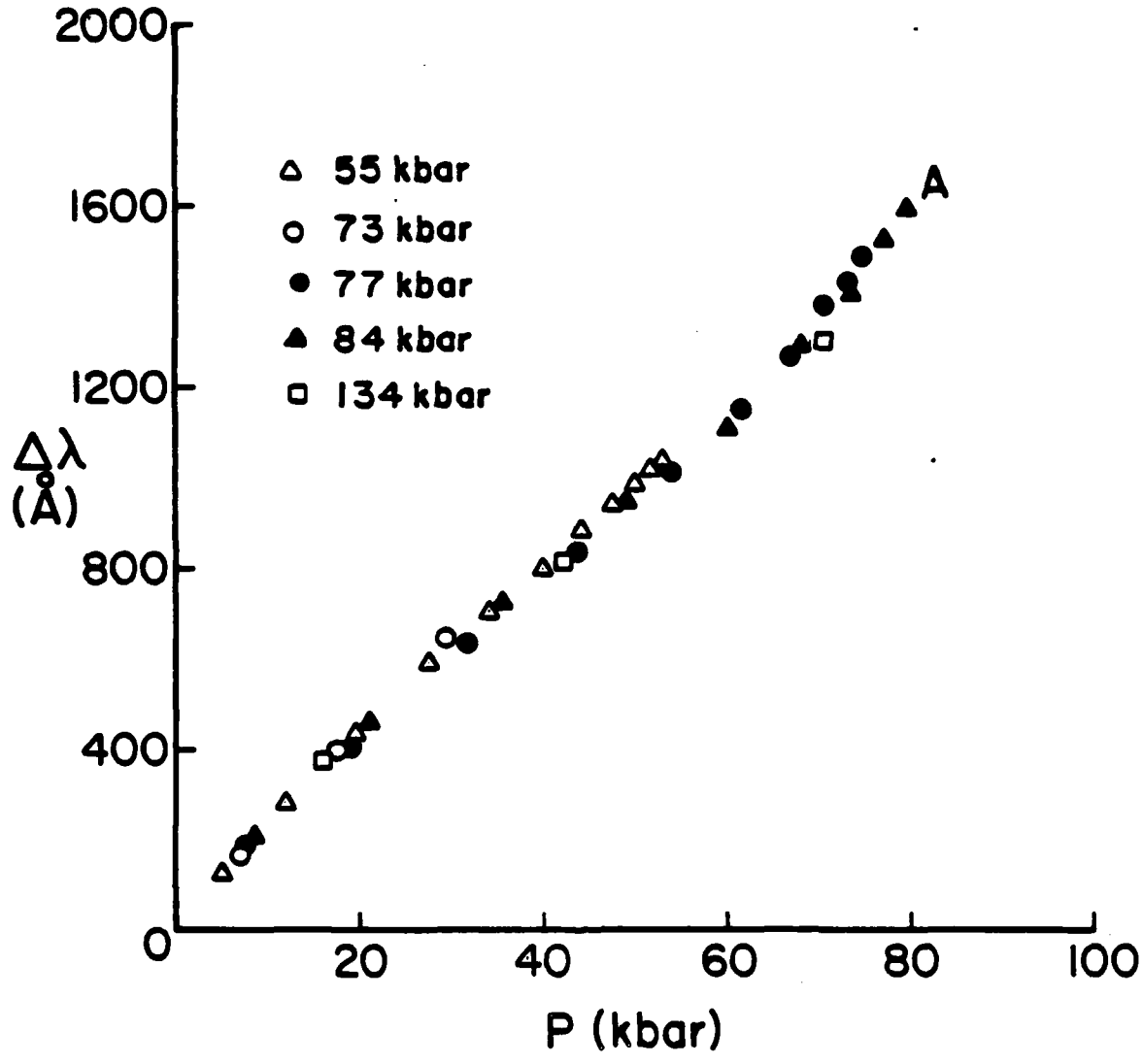

Fig. 10 Shift of red edge of 3200 Å absorption band in liquid CS_2. Thick cells and stepwise loading as in Fig. 6.

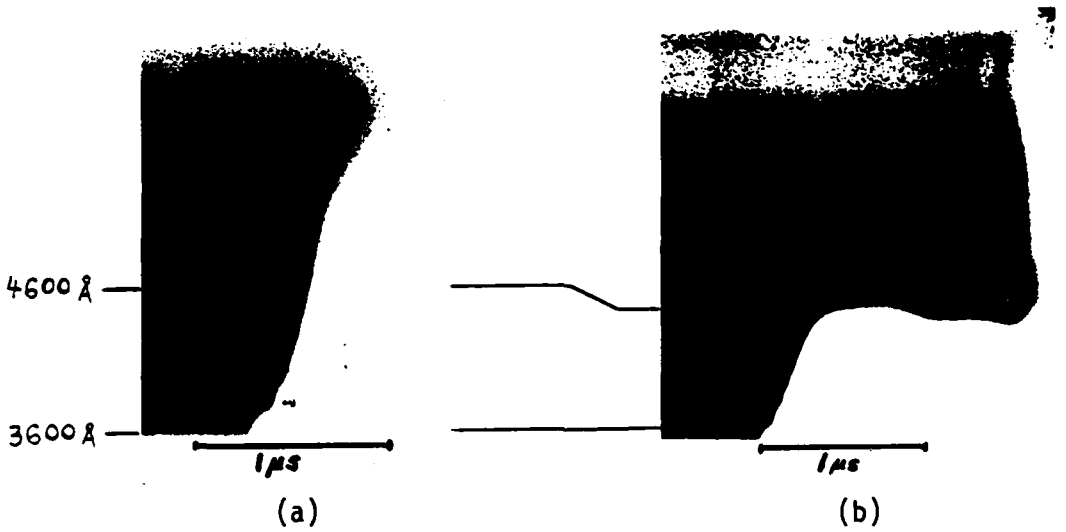

Fig. 11 Effects of Temperature on Band Edge Shift in Shocked Liquid CS_2. SW Loading (a) 67 kb, T_o = 125°C (b) 63 kb, T_o = - 72°C.[2]

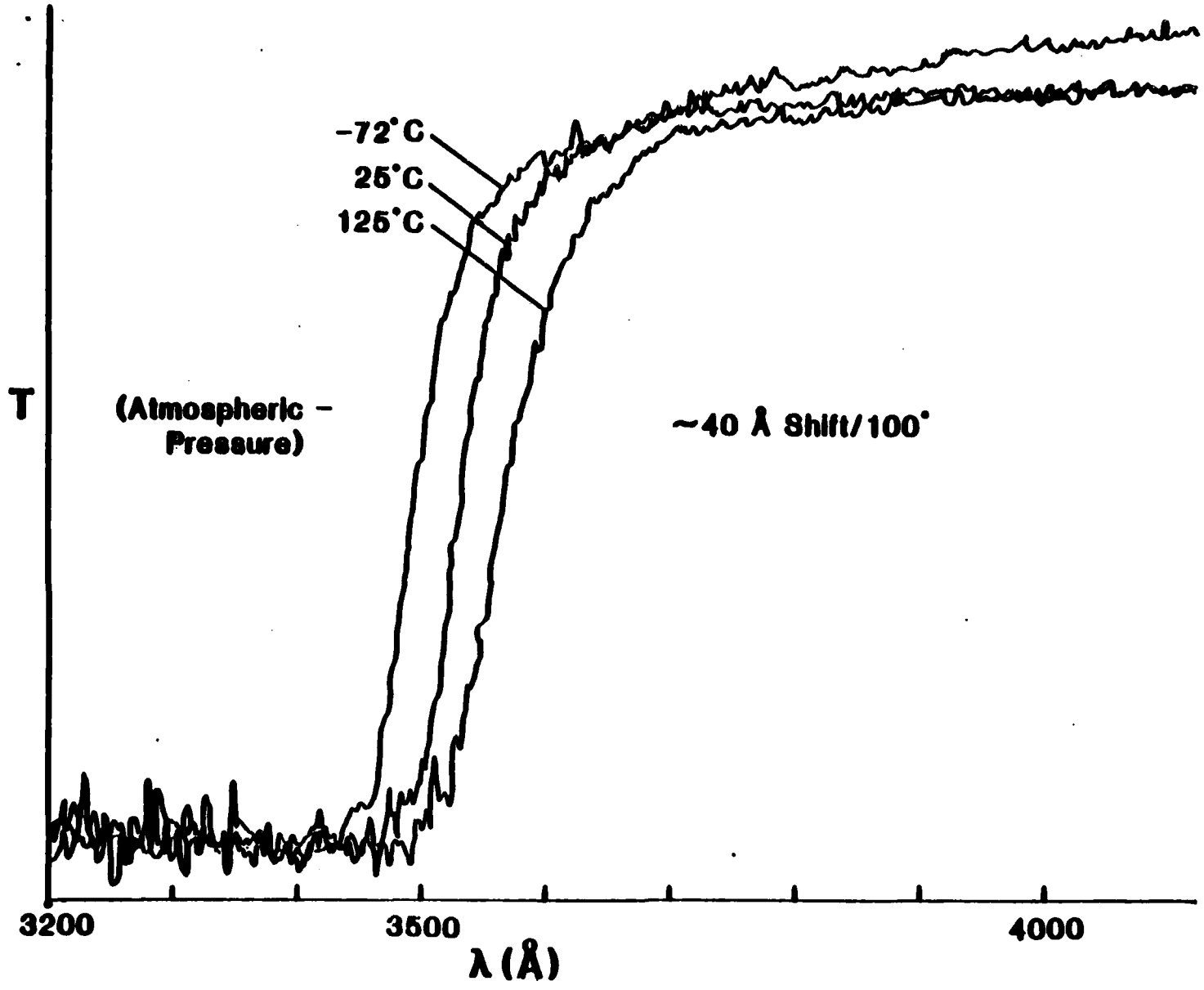

Fig. 12 Liquid CS_2 Spectrum Showing Red Edge of Absorption Band

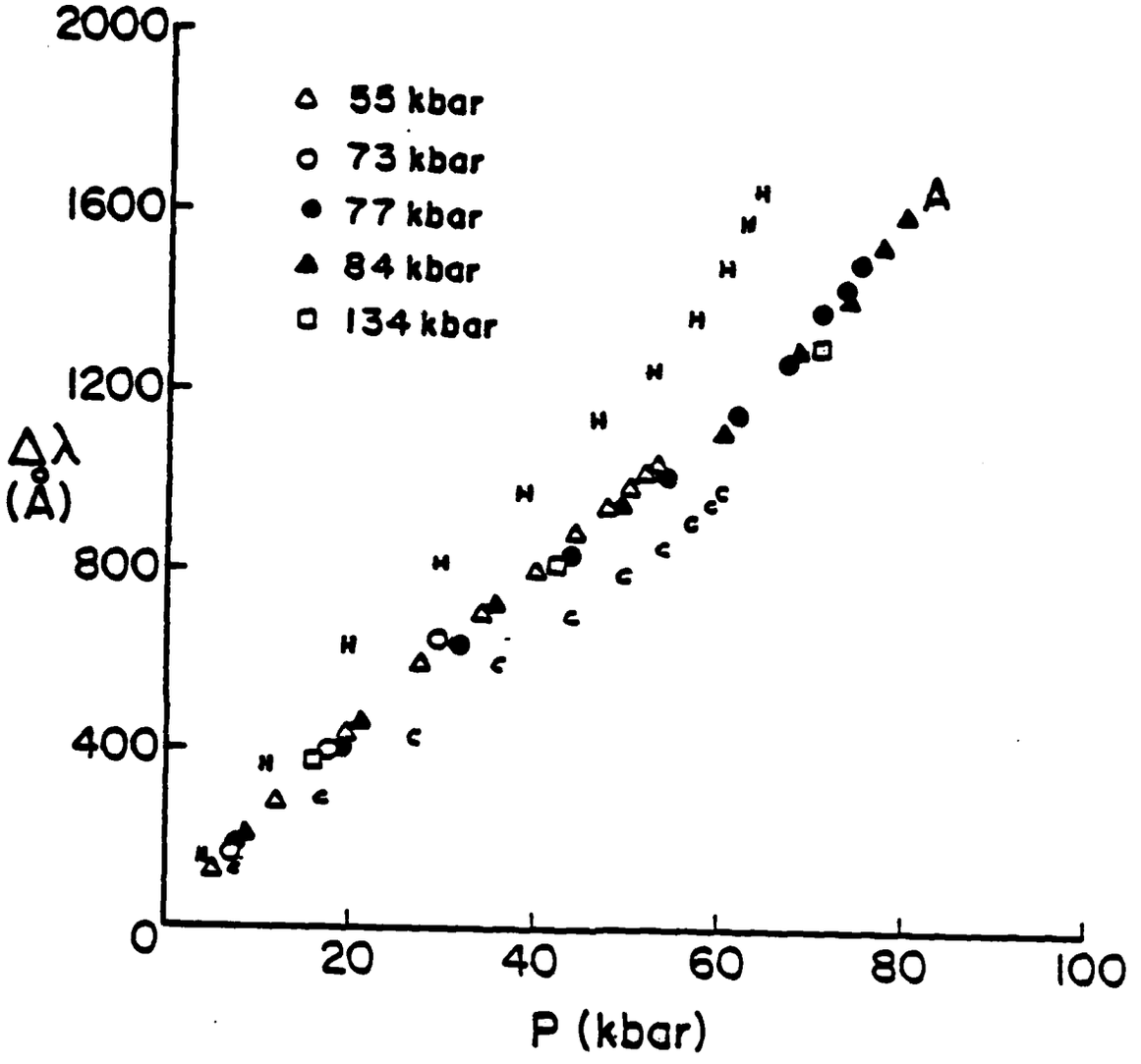

Fig. 13. Effects of Changing Initial CS_2 Temperature on Red Band Edge Shift. H: T_0 = 125°C; C: T_0 = -72°C.

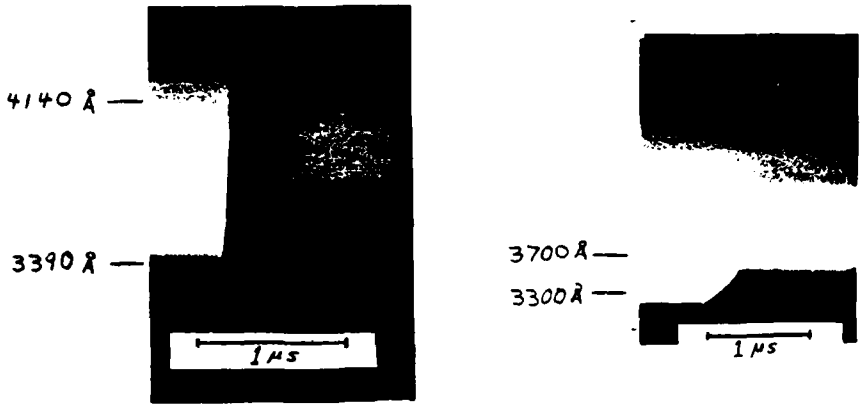

(a)

(b)

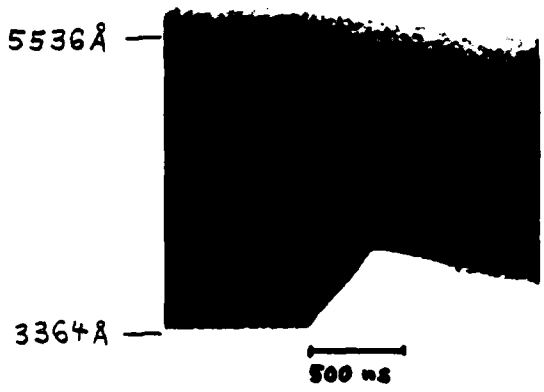

(c)

Fig. 14 Dynamic Isentropic Compression of CS_2. Thin cells
(a) Final pressure, P_f = 53 kb; rise time 87 nsec. 8 μm cell.
(b) P_f = 41 kb; risetime 340 nsec. 1 μm cell.
(c) P_f = 41 kb; risetime 340 nsec. 4 μm cell.

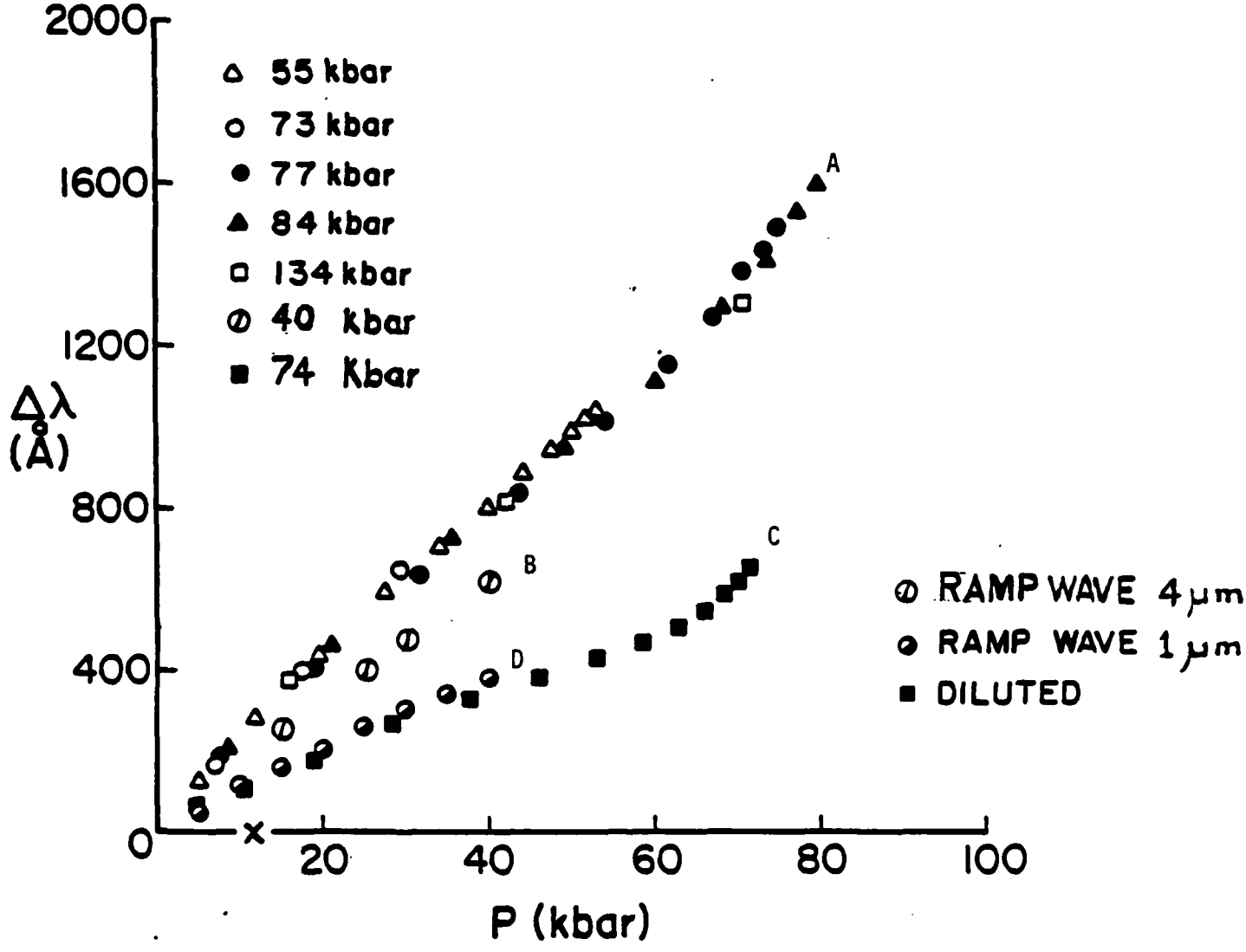

Fig. 15. Comparison of DIC and SW Loading in CS_2.

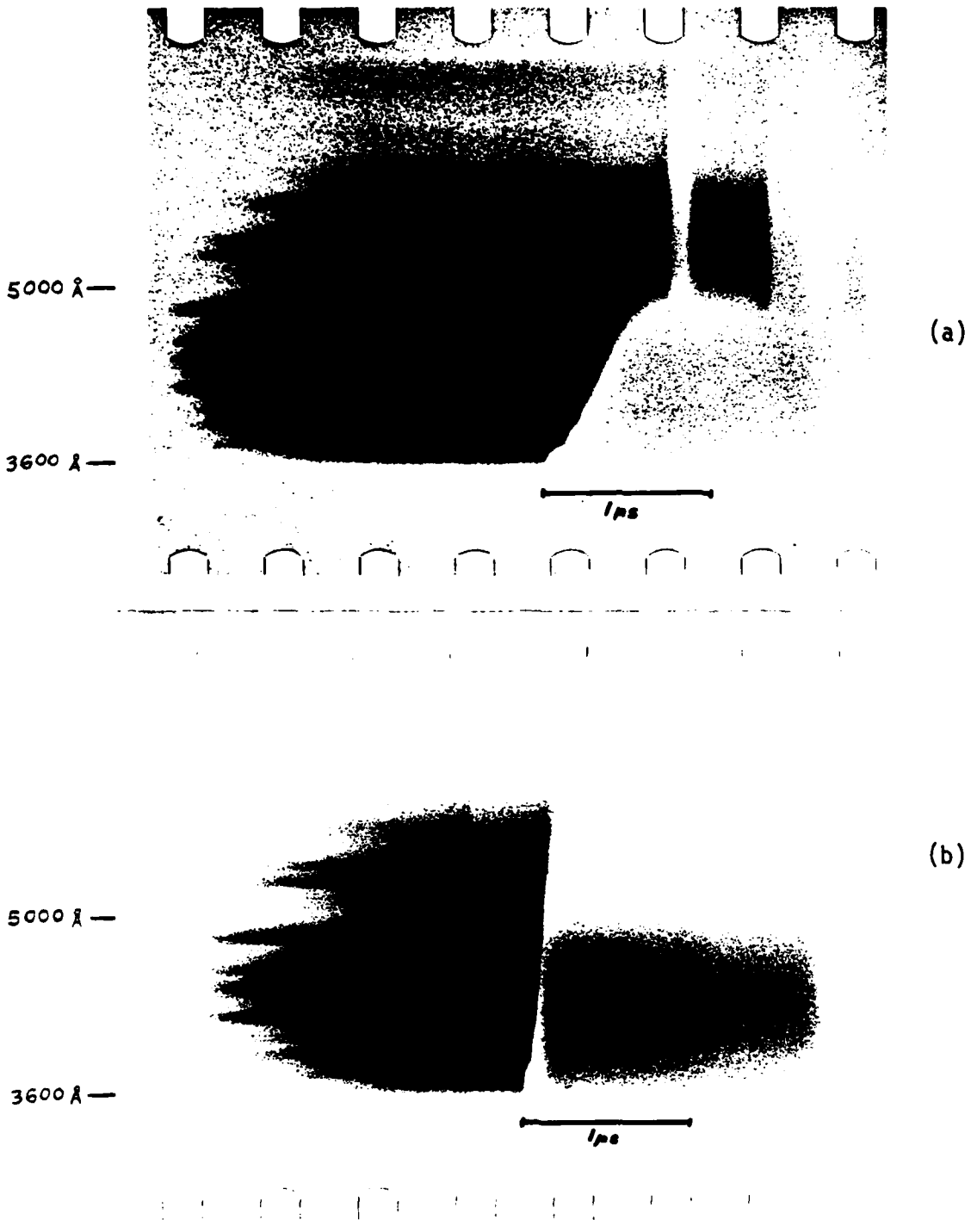

Fig. 16. Reflection Experiments in SW Loaded CS_2.
(a) 60 kbars, 193 μm; (b) 91 kb, 150 μm.

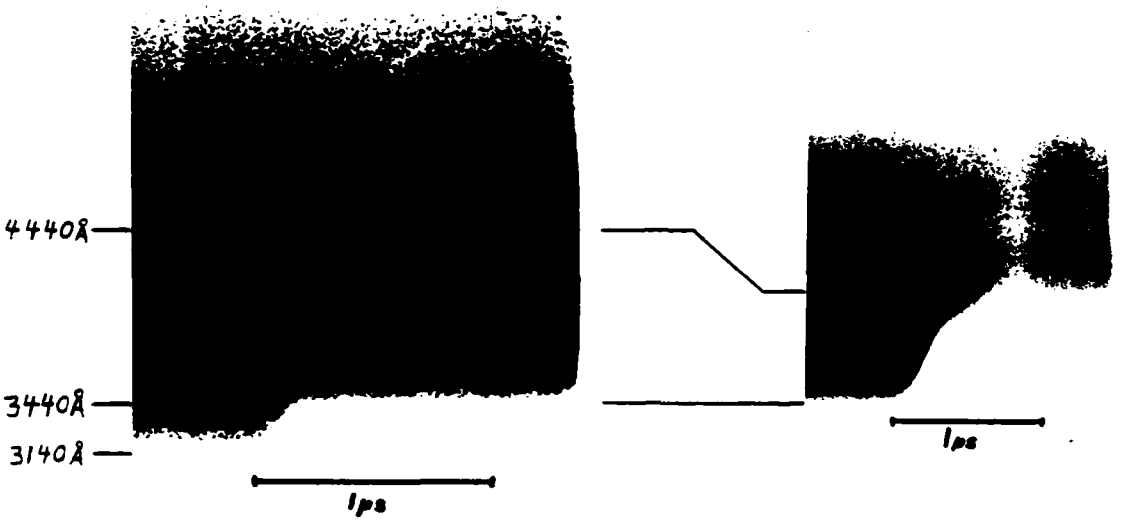

Fig. 17 SW Loading in Liquids. (a) Nitromethane, 123 kb; (b) 1/3 - CS_2/ethanol, 74 kb.

TABLE I

Shock Wave Spectroscopy Experiments 1982-83

Shot No.	Impact Pressure P_i, kb	λ_o Å	λ_1 Å	Cell Thickness μm	Rise Time nsec	Final Pressure kbars	Comments
		Group 1. Thick Cell, SW Loading, CS_2 Samples					
82-015	73	3320	4350	180	386[b]	a	
82-031	55	2700	6790	165	440	a	
82-028	77	2700	6790	116	240	a	
82-037	84	2900	6990	160	298	a	
82-018	93	2830	6920	157	274	a	
82-039	123	3210	7300	152	209	a	
83-014	134	2950	7040	158	206	a	UV filter
		Group 2. Ramp Experiments (isentropic compression, DIC), CS_2					
82-006	23	2530	4590	8	87[c]	53[d]	
83-021	27	2850	6940	1	338[c]	41[e]	
83-042	27	2658	6740	4	338	41[e]	
		Group 3. Reflection Experiments, CS_2, SW loading					
83-020	60	2910	7000	193	492		
83-019	91	2870	6980	150	265		
		Group 4. Effects of initial temperature variation, CS_2, SW loading					
83-022	67	2870	6960	164	408		T_o = 125°C
83-031	63	2920	7010	158	357		T_o = -72°C
		Group 5. Other Materials, SW Loading					
82-036	123	2300	6390	107	160		nitromethane
83-015	74	2910	7000	155	330		1/3 CS_2/ ethanol

a. Same as impact pressure.
b. Time to reach 95% of final pressure
c. Calculated from Barker's expression for sound velocity in fused quartz (70BI), see text.
d. Sapphire impactor.
e. Fused quartz impactor.

END

FILMED

3-84

DTIC